 Human Molecular Genetics, 1999, Vol. 8, No. 9 **1665–1671**

Null mutation of the murine *ATP7B* (Wilson disease) gene results in intracellular copper accumulation and late-onset hepatic nodular transformation

Olesia I. Buiakova[4], Jin Xu[4], Svetlana Lutsenko[6], Scott Zeitlin[3], Kamna Das[2], Shonit Das[5], Barbara M. Ross[2], Constantinos Mekios[1], I. Herbert Scheinberg[5] and T. Conrad Gilliam[1,2,4,+]

[1]Department of Genetics and Development, [2]Department of Psychiatry, [3]Department of Pathology and [4]Columbia Genome Center, Columbia University, [5]The National Center for the Study of Wilson's Disease and St Luke's Roosevelt Hospital, New York, NY 10032, USA and [6]Department of Biochemistry and Molecular Biology, School of Medicine, Oregon Health Science University, Portland, OR 97201, USA

Received February 28, 1999; Revised and Accepted June 7, 1999

The Atp7b protein is a copper-transporting ATPase expressed predominantly in the liver and to a lesser extent in most other tissues. Mutations in the *ATP7B* gene lead to Wilson disease, a copper toxicity disorder characterized by dramatic build-up of intracellular hepatic copper with subsequent hepatic and neurological abnormalities. Using homologous recombination to disrupt the normal translation of *ATP7B*, we have generated a strain of mice that are homozygous mutants (null) for the Wilson disease gene. The *ATP7B* null mice display a gradual accumulation of hepatic copper that increases to a level 60-fold greater than normal by 5 months of age. An increase in copper concentration was also observed in the kidney, brain, placenta and lactating mammary glands of homozygous mutants, although milk from the mutant glands was copper deficient. Morphological abnormalities resembling cirrhosis developed in the majority of the livers from homozygous mutants older than 7 months of age. Progeny of the homozygous mutant females demonstrated neurological abnormalities and growth retardation characteristic of copper deficiency. Copper concentration in the livers of the newborn homozygous null mutants was decreased dramatically. In summary, inactivation of the murine *ATP7B* gene produces a form of cirrhotic liver disease that resembles Wilson disease in humans and the 'toxic milk' phenotype in the mouse.

INTRODUCTION

Copper is a trace element and an essential cofactor for a number of enzymes that mediate vital cellular processes including mitochondrial energy generation, iron uptake regulation, melanin formation, oxygen radical scavenging, and collagen and elastin cross-linking. Although its redox properties are essential for cell function, the same properties are toxic in unbound copper. Free copper can cause damage when the total concentration exceeds the capacity of cellular copper-buffering systems. Thus, the regulation of copper homeostasis and the trafficking of intracellular copper are under tight control. Several proteins involved in copper uptake, trafficking and efflux were identified recently in yeast and mammals (1). Two human copper-transporting ATPases (2–7) recently have been identified, which are highly homologous to a single Ccc2 protein in yeast (8), and which apparently participate in copper efflux and in the delivery of copper to specific cuproproteins (9–12). Inactivation or impairment of the X-linked *ATP7A* gene results in Menkes disease in hemizygous males (13). The syndrome manifests as a severe copper deficiency disorder that presumably arises when intestinal cells are unable to transport absorbed copper to the blood stream for distribution to other organs. Mutations in the *ATP7B* gene cause Wilson disease (14,15), an autosomal recessive disorder characterized by copper accumulation in a number of tissues, but primarily in the liver, leading to hepatitis and/or cirrhosis (16,17). Although hepatic pathology is common for all patients with Wilson disease, ~40% of cases also manifest neurological and/or psychiatric disorders. Hematological, renal and endocrine forms of the disease are also described, but are much less common (17).

Two rodent strains recently have been reported that appear to bear naturally occurring mutations in the *ATP7B* gene (18,19). Long Evans Cinnamon (LEC) rats harbor an extensive deletion in the 3' portion of the gene, while 'toxic milk' mice harbor a putative point mutation in the 3' end of the gene that alters a conserved residue in the last membrane-spanning domain of the protein. Both strains are characterized by hepatic copper accumulation and liver damage (20–23), though other phenotypic manifestations of Wilson disease, including neurological, psychiatric (behavioral) and endocrine pathologies, have not been reported.

Although it appears very likely from previous studies that the naturally occurring 'toxic milk' mutation is indeed a murine model for Wilson disease, it is not clear that the muta-

[+]To whom correspondence should be addressed at: Columbia Genome Center, 1150 St Nicholas Avenue, 5th floor, New York, NY 10032, USA. Tel: +1 212 304 7984; Fax: +1 212 304 5515; Email: tcg1@columbia.edu

tion in this strain abolishes the expression of functional Atp7b protein. *ATP7B* mRNA levels are not altered in the 'toxic milk' mice (19); however, neither levels nor activities of the corresponding protein have been evaluated. The relatively mild phenotype of the 'toxic milk' mice might be attributable to residual copper-transporting activity from the protein product of the 'toxic milk' allele. It was shown recently that *ATP7B* harbors a cell type-specific promoter downstream of exon 8. The downstream promoter generates a presumptive ATPase, designated PINA (pineal night-specific ATPase). PINA is expressed specifically in the retina and pineal gland where its expression level is correlated with circadian rhythm (24). Although the precise structure of PINA has not yet been reported, it is likely that LEC and 'toxic milk' mutations, located at the 3' end of the gene, also affect the PINA transcript. If this were the case, the LEC and 'toxic milk' phenotypes would presumably reflect alterations in both *ATP7B* and PINA functions. The *ATP7B* knockout described in this study was designed to leave PINA intact. Herein we report the generation and phenotypic characterization of a murine *ATP7B* null strain. The null strain produces no detectable full size protein product of the *ATP7B* gene. The recombinant *ATP7B* allele seems to bear no mutations in the structural or regulatory elements of the PINA, an alternative shorter product of the *ATP7B* gene.

RESULTS

Generation of a null allele of the mouse *ATP7B* (Wilson disease) gene

We sought to introduce an early termination codon in the mouse *ATP7B* mRNA by engineering the substitution of a portion of *ATP7B* exon 2 with a neomycin cassette oriented in the opposite transcriptional frame. By performing homologous recombination in embryonic stem (ES) cells, the scheme was designed to preserve intron–exon boundaries while introducing multiple stop codons in all three possible reading frames (Fig. 1A). If recombinant pre-mRNA were spliced normally, the mature transcript would retain the modified exon 2 with stop codons. If, however, the modified exon 2 were alternatively spliced as indicated in Figure 2A, a frameshift mutation would be generated.

To distinguish between the two mRNA splicing scenarios, we performed RT–PCR on RNA isolated from homozygous mutant (–/–) and wild-type (+/+) animals. A variety of tissues were used to isolate RNA with identical results (data not shown). A PCR fragment, generated with primers skip.F and skip6.R (see Materials and Methods) and cDNA from mutant (–/–) liver, was sequenced. The DNA sequence confirmed that exon 2 is absent and the alternative transcript contains the intact constitutive splice sites of exons 1 and 3 (data not shown). This PCR fragment was radiolabeled and hybridized to a northern blot containing RNA isolated from the livers of homozygous mutant (Fig. 2B, lane 1) and wild-type (lane 2) mice. In both cases, a single species of RNA was detected; however, the product detected from wild-type animals is ~1.2 kb longer (the size of murine exon 2) than the corresponding RNA from mutant mice (Fig. 2B). Thus, northern hybridization results confirm that an alternative transcript lacking

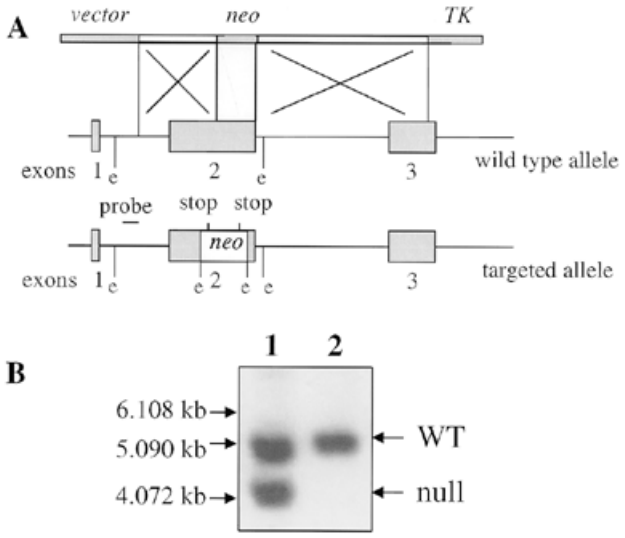

Figure 1. Strategy to target the *ATP7B* locus. (**A**) Schematic representation of the *ATP7B* targeting vector (top), the corresponding portion of the murine *ATP7B* locus (middle) and the expected recombination events (bottom). Successful integration of the targeting vector results in the deletion of a portion of exon 2 that encodes a segment of the metal-binding domain, and the insertion of a PGK-neo selection cassette encoding multiple stop codons. The location of the DNA probe used to identify putative targeted ES cell clones is indicated. (**B**) Southern blot analysis of gene targeting at the *ATP7B* locus. A 5.090 kb *Eco*RI fragment, indicative of the wild-type allele, is the sole band detected in the parental ES cell line (lane 2). An additional fragment of 4.072 kb corresponding to the targeted allele is detected in ~10% of the selected colonies (lane 1).

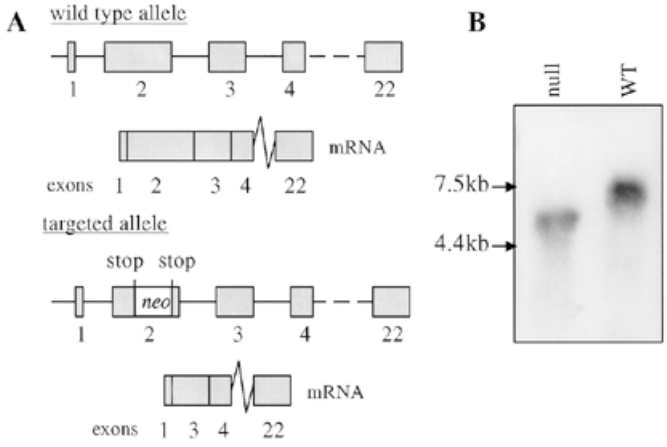

Figure 2. Expression of the wild-type and targeted *ATP7B* alleles. (**A**) Schematic representations of the intron–exon structure and corresponding mRNAs for wild-type (top) and targeted (bottom) alleles. (**B**) Northern hybridization of total RNA from null and wild-type (WT) livers. A PCR fragment containing a part of exon 1, all of exons 3, 4 and 5 and a part of exon 6 was used as probe. Note that in both cases single hybridization bands were detected. The size difference between the two bands is consistent with the absence of exon 2 (1207 bp) in the mutant message.

exon 2 is the predominant species of *ATP7B* RNA in the homozygous knockout mice.

In order to determine whether the mutant RNA can be translated into protein, we performed western blot analysis using membrane fractions isolated from the brains of wild-type, heterozygous and homozygous mutant animals. For these experiments, we used

Table 1. Copper concentrations in tissue from wild-type and mutant mice

Genotype:	Wild-type (+/+)		Mutant (–/–)				
Age:	2–4 days	2–9 months[a]	2–4 days	1 month	2 months	5 months	>7 months
Liver	249.5 ± 54.3	17.4 ± 6.2	8.1 ± 1.3	459 ± 141	905 ± 259	1021 ± 418	696 ± 438
	(*n* = 4)	(*n* = 16)	(*n* = 8)	(*n* = 3)	(*n* = 11)	(*n* = 4)	(*n* = 4)
Kidney		15.4 ± 2.8		18.8 ± 5.5	23.5 ± 3.1	53	47.0 ± 24.0
		(*n* = 9)		(*n* = 3)	(*n* = 5)	(*n* = 1)	(*n* = 3)
Brain		14.5 ± 5.0		12.6 ± 6.8	16.7 ± 3.6	26	36 ± 4
		(*n* = 9)		(*n* = 3)	(*n* = 5)	(*n* = 1)	(*n* = 3)
Eye		5.0 ±1.7		3.7 ± 0.4			
		(*n* = 4)		(*n* = 3)			

Copper levels are expressed as μg/g dry weight. In each cell, the sample mean and sample standard deviation of the measurements is given (mean ± SD), along with the sample size (n).

[a]Wild-type mice other than newborns (2–4 days old) were not subdivided into specific age groups, as there were no statistically significant differences in copper concentration between these groups.

polyclonal antibodies raised against the recombinant ATP-binding domain of the human Atp7b protein (see Materials and Methods). As shown in Figure 3, the human-derived antibody reveals a 160 kDa band (see arrow) in wild-type mice that is undetectable in homozygous mutant (–/–) mice. The mobility of the 160 kDa band matches that of the product produced in *ATP7B*-transfected COS cells (data not shown), thereby indicating that the 160 kDa band is indeed the Atp7b protein. Two non-specific bands of 110 and 130 kDa are present in all the samples regardless of the genotype. The antibodies cross-react strongly with the 110 and 130 kDa proteins in mouse tissues, but not in human tissues. Pre-incubation of the antibodies with purified recombinant ATP-binding domain prepared from Na,K-ATPase (also a P-type ATPase) does not affect the intensity of the 110 and 130 kDa bands; however, pre-incubation with tissue homogenates prepared from LEC rat hepatocytes does significantly decrease the 110 and 130 kDa band intensity (data not shown). Neither pre-incubation alters the intensity of the 160 kDa band, thus providing further support that the 160 kDa band represents the Wilson protein. The data shown in Figure 3 were obtained without subjecting antibodies to pre-adsorption protocols in order to confirm that equal amounts of protein were loaded in each lane of the gel. The data indicate that the modified *ATP7B* gene in homozygous mutant mice fails to produce the full size protein product.

Table 2. Copper concentration in lactating mammary glands, milk and placenta

	Wild-type (+/+)	Mutant (–/–)
Lactating mammary gland	4.0 ± 0.6 (*n* = 3)	9.7 ± 3.5 (*n* = 3)
Milk	15.5 ± 4.4 (*n* = 3)	5.5 ± 0.8 (*n* = 8)
Placenta (18th day of gestation)	9.5 ± 2.3 (*n* = 6)	36 ± 14 (*n* = 4)

Milk was recovered from the stomachs of 2- to 4-day-old pups.
Copper levels are expressed as μg/g dry weight. In each cell, the sample mean and sample standard deviation of the measurements is given (mean ± SD), along with the sample size (*n*).

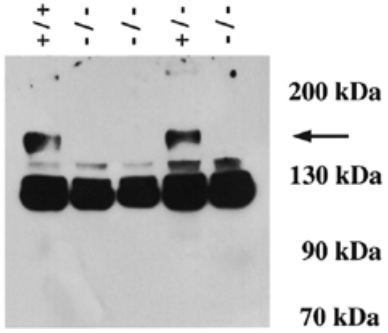

Figure 3. Western blot analysis of membrane preparations from wild-type and mutant mice. Crude membrane fractions from whole brains of wild-type (+/+), homozygous (–/–) and heterozygous (+/–) mutant mice were prepared as described in Materials and Methods. Equal amounts of protein (30 μg) were loaded onto each lane. Atp7b protein was detected using polyclonal antibody generated against the ATP-binding domain of the human Atp7b protein (a-ABD, dilution 1:20 000). An arrow indicates the position of the protein.

Phenotypic characterization of homozygous mutant mice

The dramatic accumulation of copper in liver and, to a lesser extent, other tissues is a hallmark characteristic of patients with Wilson disease. To evaluate the phenotypic consequences of the *ATP7B* gene knockout, we measured the copper concentration in liver, brain, eye, kidney (Table 1) and lactating mammary glands (Table 2) of wild-type and homozygous mutant animals.

Liver. As shown in Table 1, hepatic copper concentrations vary during the lifespan of both wild-type and mutant animals. In wild-type animals, copper concentrations peak during the first few days of postnatal life, followed by a decrease until a steady-state level is reached at ~1 month of age. We observed no significant differences in copper concentration among wild-type mice ranging from 2 to 9 months of age (data not shown). In contrast, *ATP7B* null mice are characterized by dramatically low copper concentrations at birth, followed by a gradual increase until ~2 months of age, at which point copper levels appear to reach steady state.

Compared with adult wild-type controls (2–9 months; Table 1), hepatic copper in null mice was elevated 27-fold by 1 month of age and ~50-fold by 2 months of age. The mean hepatic copper concentrations in the group of 5-month-old null animals was slightly higher than in the younger adult mutants, although the difference between the groups of 2- and 5-month-old animals was not significant . The difference between adult

wild-type animals (2–9 months of age) and 1-month-old mutants was highly significant [$P = 0.0086$ by the two-sided exact Wilcoxon rank sum test (31)], as was the difference between 1- and 2-month-old groups of mutants ($P = 0.011$). Hepatic copper levels in newborn mutant mice (2–4 days) were ~30-fold less than age-matched controls (Table 1).

Despite the dramatic copper accumulation, no gross liver pathology was detected in homozygous mutant mice prior to 5 months of age. However, in most (but not all) mice older then 7 months of age, gross anatomic liver abnormalities were detected. As shown in Figure 4, the liver surface appeared irregular with protruding regenerative nodules of different sizes, indicative of cirrhosis. The dark, relatively soft regenerative nodes progress into yellow, very dense fibrotic nodes as illustrated in Figure 4. In extreme cases, virtually all the normal hepatic parenchyma is substituted by regenerative nodes.

A comparison of copper levels in kidney, brain and eye of wild-type and homozygous mutant animals is shown in Table 1. In both kidney and brain, mutant copper levels appear to increase slightly throughout adult life. Since copper accumulation in the iris (Kayser-Fleischer rings) is a very common feature in Wilson disease patients, we compared copper concentrations in the eyes of wild-type and mutant mice. No copper deposition was revealed in the eyes of the mutant mice. A slight decrease in copper concentration was detected in 1-month-old *ATP7B* knockout mice compared with 2- to 9-month-old wild-type mice, though the difference was not statistically significant.

Milk and lactating mammary glands. In Table 2, we compare the copper concentration in milk recovered from the stomachs of pups born and nursed by either wild-type or homozygous mutant dams. Milk derived from mutant dams contained 2.8 times less copper ($P = 0.018$) than milk from wild-type dams, suggesting that the process of copper delivery to milk in mice could be analogous to the process of copper efflux from hepatocytes to the bile. Indeed, both bile and milk show low levels of copper, while copper concentration in the Atp7b-deficient hepatocytes is dramatically increased. To check whether copper accumulates in the lactating mammary glands of mutant mice, we compared copper levels in glands isolated from wild-type and mutant mice. A slight (~2.4-fold) increase in copper content was detected in the mutant mammary glands (Table 2), though certainly not commensurate with that detected in the livers of mutant mice.

Placenta. To gain some insight into the process of placental copper transport in mutant mice, we measured copper concentrations in the placentas of wild-type and null females at the 18th day of gestation. Placentas from mutant females contained 36 ± 13.9 mg copper/g of dry tissue, compared with 9.46 ± 2.3 ($P = 0.0095$) in placentas from wild-type females.

Phenotypic characterization of infant mice. The first generation of male and female homozygous mutants born to *ATP7B* heterozygous mutant parents revealed no detectable phenotypic abnormalities. However, neurological symptoms (tremor, ataxia, abnormal locomotor behavior) and retarded growth were observed in the second generation of pups born to homozygous mutant dams (data not shown). Although in a few litters the majority of the pups died by the age of 3 weeks, in the remainder most of the pups survived and appeared normal by the age of 5–6 weeks. A similar 'infant syndrome' was described in the 'toxic milk' mice, where the defect was ascribed to copper deficiency in the progeny of homozygous mutant dams (26). Since the progeny of dams with toxic milk syndrome do not develop copper deficiency symptoms when weaned with normal mothers, the deficiency presumably arises from reduced copper levels in the mother's milk (26). Cross-weaning experiments were not performed with the *ATP7B* knockout mice.

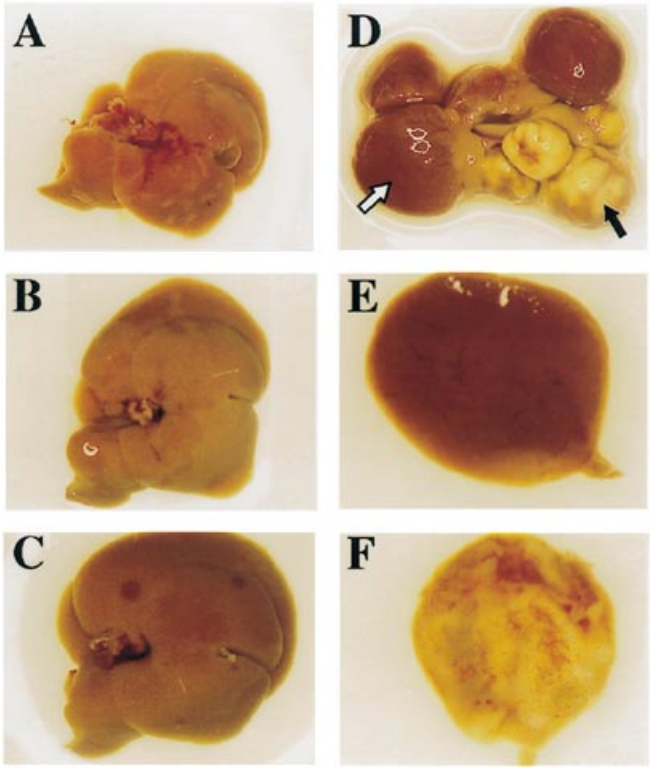

Figure 4. Crude liver pathology of livers isolated from wild-type (**A**) and 7- to 8-month-old homozygous mutant (B–D) mice. Note that mutant liver (**B**) has no regenerative nodes and is very similar to the wild-type liver (A). Liver (**C**) has a few dark red spots on its surface, which represent small regenerative nodes. The most severely affected liver (**D**) has virtually no normal parenchyma and consists of relatively new dark red regenerative nodes (white arrow, **E**) and relatively old fibrotic nodes (black arrow, **F**).

DISCUSSION

In this study, we describe the generation and preliminary characterization of a mouse strain with a homozygous mutation in the *ATP7B* gene. The mutation leads to the alternative splicing and deletion of exon 2 and the generation of a frameshift mutation at the junction of exons 2 and 3. Exon 2 encodes the N-terminus of the protein including several metal-binding sites. Western blot analysis failed to detect the full-length Atp7b protein product. We think it likely, therefore, that the targeted homologous recombination of the *ATP7B* locus generated a null allele for the Wilson disease gene.

Wilson disease is characterized by copper accumulation in various organs, primarily the liver, kidney and brain. The copper accumulation leads to morphological and functional abnormalities of these organs. The pattern of copper accumulation in

mutant mice resembles the pattern documented in untreated Wilson disease patients (16,17). Despite documented copper accumulation in various tissues, the young to middle-aged adult mice generated in this study appear to be normal. The progeny of homozygous mutant females, however, demonstrated neurological symptoms and retarded growth. A similar 'infant syndrome' was reported for the mutant pups born to homozygous mutant dams with 'toxic milk' phenotype (26), though no such symptoms have been reported in the children of mothers with Wilson disease. In the 'toxic milk' mouse, the infants' symptoms are believed to result from copper deficiency, arising, at least in part, from reduced copper levels in the milk of the mutant dams. When the same progeny are weaned with normal mothers, the copper deficiency is corrected and symptoms of the syndrome are much milder or do not develop at all. The obvious similarity between *ATP7B* null and 'toxic milk' phenotypes suggests that the A to G change in the 'toxic milk' allele is a point mutation rather than a rare polymorphism.

The knockout mutation described in this study leads to dramatic build-up of copper in the livers of young homozygous mutant mice, followed by the formation of regenerative nodes, and subsequent fibrosis, in middle- to old-aged mice. These symptoms resemble the build-up of copper and the formation of cirrhotic nodes in the livers of patients with Wilson disease. Hepatic cirrhosis is a relatively common outcome of Wilson disease. By comparison, no jaundice, ascitis or other signs of liver decompensation were observed in the mutant mice until 10 months of age. Newborn *ATP7B* mutant pups show an ~30-fold reduction in hepatic copper compared with wild-type pups. The mechanism by which hepatic copper levels are elevated during normal mammalian development is not known. Our data indicate that Atp7b is either directly or indirectly involved in this process. One possibility is that the mutant Atp7b disrupts the normal transport of copper between the mother and developing fetus, perhaps at the level of the placenta. As shown in Figure 2, copper levels in the Atp7b mutant placenta are elevated ~4-fold compared with matched controls. This is consistent with elevated expression of the *ATP7B* gene in placenta (5). The relative deficiency of hepatic copper in newborn mutant pups may reflect the defective transport of copper across the placenta, analogous to the defective transport from hepatocytes to bile and, apparently (Table 2), from mammary glands to milk. Further studies will be required to answer these questions.

The *ATP7B* null mouse described in this report should prove useful for fundamental studies of copper homeostasis. One important question to address is the functional relationship between the two highly homologous copper-transporting ATPases, Atp7a and Atp7b, in the trafficking and efflux of intracellular copper. Recent studies indicate that the expression patterns of the *ATP7B* and *ATP7A* genes largely overlap (27). The *ATP7A* gene seems to be expressed in almost all tissues, with the exception of the adult liver. *ATP7B* mRNA is expressed in most tissues, though apparently not in the embryonic liver. The patterns of copper accumulation arising from mutation of the murine *ATP7B* gene (this study) versus the *ATP7A* gene (the brindled mouse strain) (28,29), however, are quite different. The main target of copper accumulation in the *ATP7B* null mouse is the liver, while in the 'brindled' mouse the bulk of accumulated copper is found in the intestine. Nevertheless, in other organs, such as the kidneys and placenta, copper accumulation is documented in both the *ATP7B* null and 'brindled' mice. There are several possible interpretations of this phenomenon. (i) The two genes are functionally synonymous but expressed in different cell types of the same organ. In this case, copper accumulation within the organ might have different cellular patterns depending upon which ATPase is impaired. (ii) The two proteins are co-expressed in a given cell type but have distinct cellular copper trafficking roles (e.g. excretion versus reabsorption in the kidney). (iii) The two proteins are co-expressed and their biological functions are synonymous; however, neither of the ATPases is sufficient to maintain copper homeostasis in the absence of the other. Additional immunocytochemical and histochemical studies are necessary to distinguish between these possibilities.

In this study, we show that copper-deficient milk is produced by an apparently copper-laden mammary gland in *ATP7B* mutant females, suggesting a similar function for the Atp7b protein in the liver and in the lactating mammary glands. This observation identifies the murine mammary gland as an interesting tissue for the study of copper trafficking. Antibodies against known milk proteins could be used in immunohistochemical analyses to follow their trafficking and to determine whether they are co-localized with the Atp7b protein.

In conclusion, we have generated a presumptive null allele for the murine *ATP7B* gene. Our studies indicate that functional Atp7b protein is absent in the homozygous mutant animals. We provide evidence that the *ATP7B* null strain is an animal model for the hepatic form of Wilson disease, and an excellent model for study of the function of the *ATP7B* gene *in vivo*. Comparative analyses of *ATP7A* and *ATP7B* mutant mice strains may provide new clues to further our understanding of the functional relationship between these two highly homologous ATPases.

MATERIALS AND METHODS

Generation of chimeric mice

The mouse *ATP7B* targeting construct contained 3 kb of *ATP7B* sequence representing a portion of intron 1 and approximately half of exon 2, along with 5 kb of sequence representing intron 2 and the majority of exon 3. The *ATP7B* sequences were separated by a PGK-neomycin resistance (PGK-neo) insert and flanked at the 5' end by a herpes simplex virus-thymidine kinase (HSV-TK) cassette in pBluescript KS(+) (Stratagene) as illustrated in Figure 1A. The ES cell line W9.5 was grown on a feeder layer of mitomycin C-inactivated primary mouse embryonic fibroblasts in Dulbecco's modified Eagle's medium supplemented with 20% (v/v) fetal bovine serum and 0.1 mM 2-mercaptoethanol. The cells were electroporated with 25 μg of the linearized vector and clones were selected using positive (PGK-neo) and negative (HSV-TK) selection with G418 and ganciclovir, respectively. *Eco*RI-digested DNA from the surviving clones was screened for homologous recombination by Southern analysis using a probe from the 5' part of exon 2 (Fig. 1). Following verification of homologous recombination, cells from two clones were used to generate chimeric mice. Germline transmission of the targeted allele was monitored by PCR. Tail-tip DNA preparations and PCR were performed as described elsewhere (30). The wild-type *ATP7B*

allele was detected using a 5' primer homologous to DNA sequence in exon 2 (5'-GGCATTGTGAACATCAAGGTG-3') that lies outside of the 5' homology region of the targeting construct, and a 3' primer (5'-ATGGCTGTCTGCAGGAACA-3') from the part of exon 2 that is removed in the construct. The targeted allele was identified using the same 5' primer and a 3' primer (5'-TCGAGATCCACTAGTTCTAGC-3') from the 3'-untranslated region of the PGK-neo gene. A 700 bp fragment was generated in the presence of the wild-type allele and a 200 bp fragment in the presence of the targeted allele.

Detection of *ATP7B* expression

RNA was isolated from various tissues derived from wild-type and mutant mice using the RNeasy kit (Qiagen). Total RNA was then reverse transcribed using the SuperScript Preamplification System (Gibco BRL), and single-stranded cDNAs subsequently were amplified following protocols in the SuperScript Preamplification System manual.

The primers used for RT–PCR were:

Skip.F, 5'-TCACAGCCAAAGAGGCCAGT-3' exon 1;
Skip2.F, 5'-GGGAGCAATCAATGAAGCAG-3' exon 2;
Skip3.F, 5'-TGCCACAAACCATGGGTGAT-3' exon 3;
Skip4.F, 5'-TGATCCGGAGATCATCCAGT-3' exon 4;
Skip5.F, 5'-CGATCCTGAAATTGTTGGTCC-3' exon 5;
Skip2.R, 5'-TTCAGACTGGAGATCCTGTC-3' exon 2;
Skip.R, 5'-CCCAGATTTGAAGTTTCTGAC-3' exon 3;
Skip4.R, 5'-ATCAAGGCGACCAACACTGA-3' exon 4;
Skip5.R, 5'-ATGTTGTGGACACAGGAAGC-3' exon 5;
Skip6.R, 5'-CGTCTTGTGGTCCAAGTGAT-3' exon 6;
WDP.F, 5'-TCAATCTGGTGCTGGCATTG-3' exon 19;
WDP.R, 5'-AGACACTTGGCTCACGTAGC-3' exon 21.

Northern hybridization

RNA was isolated from frozen murine livers using the Qiagen RNeasy midi kit. The RNA samples, containing 5 μg of total RNA each, were run through a denaturing gel and transferred onto nytran membrane (Schleiher & Schull) as described (30). A (Skip.F/Skip6.R) RT–PCR fragment, generated with RNA from the mutant liver, was labeled with ^{32}P and used as a probe. Hybridization was performed at 68°C overnight as described previously (30).

Western blot analysis of mouse tissues

Small pieces of tissues were homogenized in 0.5–1 ml of ice-cold MTB buffer (10 mM HEPES-NaOH, 0.2 M mannitol, 50 mM sucrose, 1 mM EDTA, 10 mM KCl, pH 7.5) containing a protease inhibitor cocktail (ICN) using a glass Dounce homogenizer. Homogenates were centrifuged at 500 *g* at 4°C, for 5 min to remove tissue debris, and the membrane fraction was collected by centrifugation at 20 000 *g* at 4°C for 20 min. Pellets were resuspended in 30–150 ml of MTB buffer and 2–3 ml aliquots were taken to measure protein concentration using the Lowry method. A 100 mg aliquot of protein was collected from each sample and solubilized with Laemmli sample buffer (1:1:1 v/v of 125 mM Tris–HCl, pH 6.8, 10% SDS, 8 M urea), containing 10% β-mercaptoethanol, to reach a final protein concentration of 1 mg/ml. Then 20 ml of this solution was used for gel electrophoresis. Proteins were separated on a 7.5% Laemmli gel, transferred to PVDF membrane as described by Matsudaira (31), and immunostained with antibody directed against the recombinant ATP-binding domain of the human Wilson disease protein (antibody dilution 1:20 000). These antibodies detect the human recombinant full-length Wilson disease protein expressed in COS cells.

Quantification of copper in different tissues

Tissue samples were dried in a vacuum oven (National Appliance, III) at 70°C. The dry tissues were weighed and dissolved in concentrated HNO_3 at 60°C in a dry bath incubator (Fisher Scientific). The amount of copper present in the solution was determined by polarized atomic absorption spectrophotometry using a Hitachi Z-8279 spectrophotometer with a graphite furnace.

ABBREVIATIONS

ES cells, embryonic stem cells; HSV-TK, herpes simplex virus-thymidine kinase gene; LEC rats, Long Evans Cinnamon rats; PINA, pineal night-specific ATPase; PGK-neo, phosphoglycerate kinase-neomycin resistance gene.

ACKNOWLEDGEMENTS

We thank Harold Goring and Dr Joseph Terwilliger for assistance with the statistical evaluation of data. This work was supported in part by grant no. 5-38300 from the National Institute of Health.

REFERENCES

1. Harris, Z.L. and Gitlin, J.D. (1996) Genetic and molecular basis for copper toxicity. *Am. J. Clin. Nutr.*, **63**, 836S–841S.
2. Chelly, J., Tumer, Z., Tonnesen, T., Petterson, A., Ishikawa-Brush, Y., Tommerup, N., Horn, N. and Monaco, A.P. (1993) Isolation of a candidate gene for Menkes disease that encodes a potential heavy metal binding protein. *Nature Genet.*, **3**, 14–19.
3. Mercer, J.F.B., Livingston, J., Hall, B., Paynter, J.A., Begy, C., Chandrasekharappa, S., Lockhart, P., Grimes, A., Bhave, M., Siemieniak, D. and Glover, T.W. (1993) Isolation of a partial candidate gene for Menkes disease by positional cloning. *Nature Genet.*, **3**, 20–25.
4. Vulpe, C., Levinson, B., Whitney, S., Packman, S. and Gitschier, J. (1993) Isolation of a candidate gene for Menkes disease and evidence that it encodes a copper-transporting ATPase. *Nature Genet.*, **3**, 7–13.
5. Tanzi, R.E., Petrukhin, K., Chernov, I., Pellequer, J.L., Wasco, W., Ross, B., Romano, D.M., Parano, E., Pavone, L., Brzustowicz, L.M., Devoto, M., Peppercorn, J., Bush, A.I., Sternlieb, I., Pirastu, M., Gusella, J.F., Evgrafov, O., Penchaszadeh, G.K., Honib, B., Edelman, I.S., Soares, M.B., Schienberg, I.H. and Gilliam, T.C. (1993) The Wilson disease gene is a copper transporting ATPase with homology to the Menkes disease gene. *Nature Genet.*, **5**, 355–350.
6. Petrukhin, K., Lutsenko, S., Chernov, I., Ross, B.M., Kaplan, J.H. and Gilliam, T.C. (1994) Characterization of the Wilson disease gene encoding a P-type copper transporting ATPase: genomic organization, alternative splicing, and structure/function predictions. *Hum. Mol. Genet.*, **3**, 1647–1656.
7. Bull, P.C., Thomas, G.R., Rommens, J.M., Forbes, J.R. and Cox, D.W. (1993) The Wilson disease gene is a putative copper transporting P-type ATPase similar to the Menkes gene. *Nature Genet.*, **5**, 327–337.
8. Fu, D., Beeler, T.J. and Dunn, T.M. (1995) Sequence, mapping and distribution of *CC*C2, a gene that cross-complements the Ca^{2+}-sensitive phenotype of *csg1* mutants and encodes a P-type ATPase belonging to the Cu^{2+}-ATPase subfamily. *Yeast*, **11**, 283–292.
9. Dierick, H.A., Adam, A.N., Escara-Wilke, J.F. and Glover, T.W. (1997) Immunocytochemical localization of the Menkes copper transport protein (ATP7A) to the *trans*-Golgi network. *Hum. Mol. Genet.*, **6**, 406–416.

10. Hung, I.H., Suzuki, M., Yamaguchi, Y., Yuan, D.S., Klausner, R.D. and Gitlin, J.D. (1997) Biochemical characterization of the Wilson disease protein and functional expression in the yeast *Saccharomyces cerevisiae*. *J. Biol. Chem.*, **272**, 21461–21466.
11. Nagano, K., Nakamura, K.-I., Umeyama, K., Uchiyama, H., Koiwai, K., Hattori, S., Yamamoto, T., Matsuda, I. and Endo, F. (1998) Intracellular distribution of the Wilson's disease gene product (ATPase7B) after *in vitro* and *in vivo* exogenous expression in hepatocytes from LEC rat, an animal model of Wilson's disease. *Hepatology*, **27**, 799–807.
12. Petris, M.J., Mercer, J.F.B., Culvenor, J.G., Lockhart, P., Gleeson, P.A. and Camakaris, J. (1996) Ligand-regulated transport of the Menkes copper P-type ATPase efflux pump from the Golgi apparatus to the plasma membrane: a novel mechanism of regulated trafficking. *EMBO J.*, **15**, 6084–6095.
13. Kaler, S.G. (1996) Menkes disease mutations and response to early copper histidine treatment. *Nature Genet.*, **13**, 21–22.
14. Shah, A.B., Chernov, I., Zhang, H.T., Ross, B.M., Das, K., Lutsenko, S., Parano, E., Pavone, L., Evgrafov, O., Ivanova-Smolenskaya, I.A., Anneren, G., Westermark, K., Hevia Urritia, F., Penchaszadeh, G.K., Sternlieb, I., Scheinberg, I.H., Gilliam, T.C. and Petrukhin, K. (1997) Identification and analysis of mutations in the Wilson disease gene (*ATP7B*): population frequencies, genotype–phenotype correlation, and functional analyses. *Am. J. Hum. Genet.*, **61**, 317–328.
15. Thomas, G.R., Forbes, J.R., Roberts, E.A., Walshe, J.M. and Cox, D.W. (1995) The Wilson disease gene: spectrum of mutations and their consequences. *Nature Genet.*, **9**, 210–217.
16. Hoogenraad, T. (1996) *Wilson's Disease*. W.B. Saunders Company.
17. Scheinberg, I.H. and Sternlieb, I. (1984) *Wilson's Disease*. W.B. Saunders Company.
18. Wu, J., Forbes, J.R., Chen, H.S. and Cox, D.W. (1994) The LEC rat has a deletion in the copper transporting ATPase gene homologous to the Wilson disease gene. *Nature Genet.*, **7**, 541–545.
19. Theophilos, M.B., Cox, D. and Mercer J.F.B. (1996) The toxic milk mouse is a murine model of Wilson disease. *Hum. Mol. Genet.*, **5**, 1619–1624.
20. Mori, M., Hattori, A., Sawaki, M., Tsuzuki, N., Sawada, N., Oyamada, M., Sugawara, N. and Enomoto, K. (1994) The LEC rat: a model for human hepatitis, liver cancer, and much more. *Am. J. Pathol.*, **144**, 200–204.
21. Okayasu, T., Tochimaru, H., Takahashi, T., Takekoshi, Y., Li, Y., Togashi, Y., Takeichi, N., Kasai, N. and Arashima, S. (1992) Inherited copper toxicity in Long-Evans Cinnamon rats exhibiting spontaneous hepatitis: a model of Wilson's disease. *Pediatr. Res.*, **31**, 253–257.
22. Yoshida, M.C., Masuda, R., Sasaki, M., Takeichi, N., Kobayashi, H., Dempo, K. and Mori, M. (1987) New mutation causing hereditary hepatitis in the laboratory rat. *J. Hered.*, **78**, 361–365.
23. Biempica, L., Rauch, H., Quintana, N. and Sternlieb, I. (1988) Morphologic and chemical studies on a murine mutation (toxic milk mice) resulting in hepatic copper toxicosis. *Lab. Invest.*, **59**, 500–508.
24. Li, X., Chen, S., Wang, Q., Zack, D.J., Snyder, S.H. and Borjigin, J. (1998) A pineal regulatory element (PIRE) mediates transactivation by the pineal/retina-specific transcription factor CRX. *Proc. Natl Acad. Sci. USA*, **95**, 1876–1881.
25. Akland, M.L., Cornish, E.J., Paynter, J.A., Grimes, A., Michalczyk, A. and Mercer, J.F.B. (1997) Expression of Menkes disease gene in mammary carcinoma cells. *Biochem. J.*, **328**, 237–243.
26. Rauch, H. (1983) Toxic milk, a new mutation affecting copper metabolism in the mouse. *J. Hered.*, **74**, 141–144.
27. Kuo, Y.-M., Gitschier, J. and Packman, S. (1997) Developmental expression of the mouse mottled and toxic milk genes suggests distinct functions for the Menkes and Wilson disease copper transporters. *Hum. Mol. Genet.*, **6**, 1043–1049.
28. Mercer, J.F.B. (1998) Menkes syndrome and animal models. *Am. J. Clin. Nutr.*, **67** (Suppl.), 1022S–1028S.
29. Yoshimura, N. (1994) Histochemical localization of copper in various organs of brindled mice. *Pathol. Int.*, **44**, 14–19.
30. Ausubel, F.M., Brent, R., Kingston, R.E., Moore, D.D., Seidman, J.G., Smith, J.A. and Struhl, K. (eds) (1995) *Current Protocols in Molecular Biology*. John Wiley & Sons, New York.
31. Matsudaira, P. (1987) Sequence from picomole quantities of proteins electroblotted onto polyvinylidene difluoride membranes. *J. Biol. Chem.*, **262**, 10035–10038.
32. S-plus version 4.0; release 3 (1998) Math Soft, Inc.